Atmospheric
Chemistry
and Physics
Discussions

Open Access

EGU

# Emission of nitrous acid from soil and biological soil crusts represents a dominant source of HONO in the remote atmosphere in Cyprus

Hannah Meusel[1], Alexandra Tamm[1], Uwe Kuhn[1], Dianming Wu[1], Anna Lena Leifke[1], Sabine Fiedler[2], Nina Ruckteschler[1], Petya Yordanova[1], Naama Lang-Yona[1], Jos Lelieveld[3,4], Thorsten Hoffmann[5], Ulrich Pöschl[1], Hang Su[1,6], Bettina Weber[1], Yafang Cheng[1,6]

[1]Max Planck Institute for Chemistry, Multiphase Chemistry Department, Mainz, Germany
[2]Johannes Gutenberg University, Institute for Geography, Mainz, Germany
[3]Max Planck Institute for Chemistry, Atmospheric Chemistry Department, Mainz, Germany
[4]The Cyprus Institute, Nicosia, Cyprus
[5]Johannes Gutenberg University, Institute for Inorganic and Analytical Chemistry, Mainz, Germany
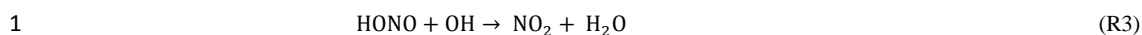[6]Institute for Environmental and Climate Research, Jinan University, Guangzhou, China

Corresponding author: Yafang Cheng (yafang.cheng@mpic.de) and Bettina Weber (b.weber@mpic.de)

**Abstract.** Soil and biological soil crusts can emit nitrous acid (HONO) and nitric oxide (NO). The terrestrial ground surface in arid and semi-arid regions is anticipated to play an important role in the local atmospheric HONO budget, deemed to represent one of the unaccounted HONO sources frequently observed in field studies. In this study HONO and NO emissions from a representative variety of soil and biological soil crust samples from the Mediterranean island Cyprus were investigated under controlled laboratory conditions. A wide range of fluxes was observed, ranging from 0.6 to 264 ng m$^{-2}$ s$^{-1}$ HONO-N at optimal soil water content (20-30% of water holding capacity, WHC). Maximum NO-N at this WHC fluxes were lower (0.8-121 ng m$^{-2}$ s$^{-1}$). Highest emissions of both reactive nitrogen species were found from bare soil, followed by light and dark cyanobacteria-dominated biological soil crusts (biocrusts), correlating well with the sample nutrient levels (nitrite and nitrate). Extrapolations of lab-based HONO emission studies agree well with the unaccounted HONO source derived previously for the extensive CYPHEX field campaign, i.e., emissions from soil and biocrusts may essentially close the Cyprus HONO budget.

## 1 Introduction

Nitrous acid (HONO) plays an important role in tropospheric chemistry, as it is one of the major precursors of the hydroxyl (OH) radical which determines the oxidizing capacity of the atmosphere. In the early morning, HONO photolysis has been shown to contribute up to 30% to the local OH budget (Alicke et al., 2002; Kleffmann et al., 2005; Ren et al., 2003 and 2006; Meusel et al., 2016). Currently, the HONO formation processes, especially during daytime, are still not fully understood. Recent ground based field measurements showed unexpected high daytime concentrations of HONO, which could not be explained by atmospheric gas phase reactions (R1-R3) only (Kleffmann et al., 2003 and 2005; Su et al., 2008a; Soergel et al., 2011a; Su et al., 2011; Michoud et al., 2014; Czader et al., 2012; Wong et al., 2013; Tang et al., 2015; Oswald et al., 2015, Meusel et al., 2016).

$$OH + NO \rightarrow HONO \tag{R1}$$

$$HONO \xrightarrow{h\nu\ (300-405\ nm)} OH + NO \tag{R2}$$

1 $$HONO + OH \rightarrow NO_2 + H_2O \tag{R3}$$

2 Several studies have shown that HONO can be heterogeneously formed from $NO_2$ on a variety of surfaces, e.g., soot,

3 humic acid, minerals, proteins and organically coated particles (Ammann et al., 1998; Arens et al., 2001; Aubin et

4 al., 2007; Bröske et al., 2003; Han et al., 2013; Kalberer et al., 1999; Kleffmann et al., 1999; Kleffmann and Wiesen,

5 2005; Lelievre et al., 2004; Kinugawa et al., 2011; Liu et al., 2015; Wang et al., 2003; Yabushita et al., 2009; Meusel

6 et al., 2017). Light can activate some of these surfaces (humic acid, proteins and other organic compounds, titanium

7 dioxide, soot), which enhances $NO_2$ uptake and HONO production (George et al., 2005; Langridge et al., 2009;

8 Monge et al., 2010; Ndour et al., 2008; Ramazan et al., 2004; Stemmler et al., 2007; Kebede et al., 2013; Meusel et

9 al., 2017). But $NO_2$ uptake coefficients and the ambient aerosol surface areas for heterogeneous reactions of $NO_2$

10 were nevertheless frequently found to be too low to account for the observed HONO production rates (Stemmler et

11 al., 2007; Sarwar et al., 2008; Zhang et al., 2016). Besides the heterogeneous $NO_2$ reaction, Bejan et al. (2006)

12 observed HONO formation during irradiation of nitrophenols. Photolysis of nitrate or nitric acid generates HONO as

13 well (Baergen and Donaldson, 2013; Scharko et al., 2014; Zhou et al., 2003, 2011). Contrary to the detected missing

14 HONO source near the ground, recent airborne measurements (500 – 1200 m above ground level) observed HONO

15 concentrations, which could be explained by gas phase reactions only (Li et al., 2014; Neuman et al., 2016).

16 However, vertical gradient studies show higher HONO concentrations near the ground than in higher altitudes

17 indicating a ground level source (Harrison and Kitto, 1994; Kleffmann et al., 2003; Ren et al., 2011; Stutz et al.,

18 2002; VandenBoer et al., 2013; Villena et al., 2011; Zhou et al., 2011; Wong et al., 2012 and 2013; Vogel et al.,

19 2003; Zhang et al., 2009; Young et al., 2012). This is supported by gas exchange studies showing that HONO and

20 NO can be emitted from (natural) soil and biological soil crusts (biocrusts, BSC), even without applying atmospheric

21 $NO_2$ (Su et al., 2011; Oswald et al., 2013; Mamtimin et al., 2016; Weber et al., 2015; Meixner and Yang, 2006).

22 HONO and NO can be formed during biological processes (nitrification and denitrification; Pilegaard, 2013), in

23 which $NH_3$ or $NH_4^+$ is oxidized stepwise or $NO_3^-$ is reduced (Fig. 1). Depending on soil-pH and according to Henry´s

24 law soil nitrite ($NO_2^-$) can be converted into gaseous HONO.

25 Biocrusts grow within the uppermost millimeters to centimeters of soil in arid and semi-arid ecosystems. They are

26 composed of photoautotrophic cyanobacteria, algae, lichens, and bryophytes, growing together with heterotrophic

27 bacteria, fungi and archaea in varying proportions (Belnap et al., 2016). Depending on the dominating

28 photoautotrophs, cyanobacteria-dominated biocrusts with an initial thin light-colored and a well-developed dark

29 type, cyanolichen- and chlorolichen-dominated biocrusts with lichens comprising cyanobacteria or green algae as

30 photobionts, and bryophyte-dominated biocrusts are distinguished (Büdel et al., 2009). Many free living

31 cyanobacteria but also those in symbiosis with fungi (forming lichens) and vascular plants can fix atmospheric

32 nitrogen $N_2$ and convert it into ammonia (Cleveland et al., 1999; Belnap 2002; Herridge et al., 2008; Barger et al.,

33 2016). Globally it is estimated that 100-290 Tg (N) $yr^{-1}$ is fixed biologically (Cleveland et al., 1999), of which 49 Tg

34 $yr^{-1}$ (17-49%) is fixed by cryptogamic covers, which comprise biocrusts, but also other microbially dominated

35 biomes, like lichen and bryophyte communities occurring on soil, rocks and plants in boreal and tropical regions

36 (Elbert et al., 2012). Studies hav suggested, that nitrogen cycling in soil ($N_2$ fixation, nitrification, denitrification)

37 and hence reactive nitrogen emission (NO, $N_2O$, HONO) is often enhanced by well-established biocrusts, especially

Atmospheric
Chemistry
and Physics
Discussions

1    by dark cyanobacteria (Cleveland et al., 1999; Elbert et al., 2012; Belnap, 2002; Barger et al., 2013; Johnson et al.,

2    2005; Abed et al., 2013; Strauss et al., 2012; Weber et al., 2015).

3    In Cyprus, an island in the semi-arid eastern Mediterranean area, biocrusts are ubiquitously covering ground surfaces

4    and hence can be anticipated to play an important role in the local HONO budget. In the CYPHEX campaign 2014

5    (CYprus PHotochemical EXperiment) the observed diel cycles of HONO ambient air concentrations revealed strong

6    unaccounted sources of HONO and NO, being well correlated with each other (Meusel et al., 2016). With low $NO_2$

7    concentrations and high $HONO/NO_x$ ratios, respectively, direct emissions from combustion and heterogeneous

8    reactions of $NO_2$ could be excluded as significant HONO sources, leaving emissions from soil and the respective

9    surface cover to be the most plausible common source for both nitrogen species (Meusel et al., 2016).

10    In the present study we measured HONO and NO fluxes from soil and biocrust samples from Cyprus by means of a

11    dynamic chamber system. The aim of this study was to characterize and quantify direct trace gas emissions and

12    demonstrate their impact on the atmospheric chemistry in the remote coastal environment of Cyprus.

13    **2 Methods**

14    **2.1 Sampling**

15    Bare soil and biocrust samples were collected on 27th April 2016 on the South/South-East side of the military station

16    in Ineia, Cyprus (34.9638°N, 32.3778°E), where the CYPHEX campaign took place in 2014. It is a rural site about

17    600 m above sea level, approximately 5-8 km from the coast and is surrounded by typical Mediterranean vegetation

18    (olive and pine trees, small shrubs like *Pistacia lentiscus, Sacopoterium spinosum* and *Inula viscosa).* More details

19    about the site can be found in Meusel et al. (2016).

20    In an area of about 8580 m² (South/South-East direction of the station) 50 grids (25x25 cm) were placed at randomly

21    selected spots for systematic ground cover assessment. At each grid point occurrence of nine types of surface cover

22    (i.e., light and dark cyanobacteria-, chlorolichen-, cyanolichen-, and moss-dominated biocrust, bare soil, stone, litter,

23    vascular vegetation/shrub) were assigned and quantified. Spatially independent replicate samples were collected of

24    light cyanobacteria-dominated biocrusts (light BSC), dark cyanobacteria-dominated biocrusts with cyanolichens

25    (dark BSC), chlorolichen-dominated biocrusts (chlorolichen BSC I, chlorolichen BSC II), moss-dominated biocrusts

26    (moss BSC) and of bare soil (Fig. S1 of the supplement). Each sample was collected in a plastic petri dish, sealed

27    and stored in the dark at room temperature until further analysis (storage time less than 15 weeks).

28    In total 43 samples were collected (Table 1) of which 18 samples, i.e., 3 replicates of each HONO emitting surface

29    cover type were used direct (upfront) for nutrient analysis, while all others were first used for trace gas exchange

30    measurements, prior to nutrient and chlorophyll content analysis.

31    **2.2 Meteorological data**

32    During CYPHEX the meteorological parameters were even measured at about 5 m above ground, considered not

33    representative for the micro-habitat of the soil ground surface. Hence we placed three humidity (and temperature)

34    sensors (HOBO Pro v2) just on top of the soil surface about 4 weeks prior to sample collection. Reference

35    meteorological data (air temperature, humidity and precipitation) from Paphos airport (about 20 km south of the

1    sample area, 12 m asl) and Prodromos (about 40 km east of the sampling area, 1380 m asl) during the sampling

2    period as well as the precipitation data from the last 4 years (2013-2016) were provided by the Department of

3    Meteorology,                                                                                          Cyprus

4    (http://www.moa.gov.cy/moa/ms/ms.nsf/DMLmeteo_reports_en/MLmeteo_reports_en?opendocument;  last  access:

5    Dec. 2016).

6    **2.3 Soil characteristics: nutrient, chlorophyll and pH**

7    Soil characteristics (nutrient, pH) have an effect on soil emission, e.g., higher nutrient level and lower pH would

8    enhance emission according to Henry law (Su et al., 2011). Nutrient analysis was conducted on samples without gas

9    exchange measurements (n = 3) and on replicate samples after gas exchange measurements in order to analyze

10   potential effects of the applied 'wetting-drying' cycle. Nitrate ($NO_3^-$), nitrite ($NO_2^-$) and ammonium ($NH_4^+$) were

11   analyzed via flow injection analysis with photometric detection (FIAstar 5000, Foss, Denmark). Prior to that, the

12   samples comprised of soil and its biocrust-cover were gently ground and an aliquot of 7 g was solved in 28 mL of

13   0.0125 M $CaCl_2$. After shaking for 1 hour the mixture was filtered on a N-free filter.

14   Chlorophyll analysis, as an indicator of biomass of photo-autotrophic organisms, was done according to the dimethyl

15   sulfoxide (DMSO) method (Ronen and Galun, 1984). Ground samples were extracted twice with $CaCO_3$ saturated

16   DMSO (20 mL, 10 mL) at 65°C for 90 min. Both extracts were combined and centrifuged (3000 G) at 15°C for 10

17   min. The light absorption at 648, 665 and 700 nm was detected with a spectral photometer (Lambda 25 UV/VIS

18   Spectrometer, Perkin Elmer, Rodgau). The amount of chlorophyll a ($Chl_a$) was calculated according to Arnon et al.

19   (1974). Chlorophyll a+b ($Chl_{a+b}$) content was calculated according to Lange, Bilger and Pfanz (pers. comm. in Weber

20   et al., 2013):

21    $$Chl_{a+b}[\mu g] = \left(20.2 \cdot (E_{648} - E_{700}) + 8.02 \cdot (E_{665} - E_{700})\right) \cdot a \qquad (eq.1)$$

22    $$Chl_a[\mu g] = \left(12.19 \cdot (E_{665} - E_{700})\right) \cdot a \qquad (eq.2)$$

23   where $Chl_{a+b}[\mu g]$, $Chl_a[\mu g]$ is the chlorophyll content of the sample, $E_{648}$, $E_{665}$, $E_{700}$ are light absorption at the given

24   wavelength, and a is the amount of DMSO used in mL.

25   The pH was determined for each surface cover type (n = 3-4) according to Weber et al. (2015, Suppl.). Here, 1.5 g of

26   the ground sample was mixed with 3.75 mL of pure water and shaken for 15 min. Then the slurry was centrifuged

27   (3000 G, 5 min) to separate the solid phase from the liquid solution. The latter was used for pH determination by

28   means of a pH electrode (Inlab Export Pro-ISM, Mettler Toledo).

29   **2.4 Trace gas exchange measurements**

30   The dynamic chamber method for analyzing NO and HONO emissions from soil samples was already introduced

31   before (Oswald et al., 2013; Weber et al., 2015; Wu et al., 2014). Soil and biocrust samples (25-35 g) were wetted

32   with 8-13 g of pure water (18.2 MΩ) up to water holding capacity and placed into a dynamic Teflon film chamber

33   (≈47 L) flushed with 8 L min$^{-1}$ dry pure air (PAG 03, Ecophysics, Switzerland). Typical drying cycles lasted between

34   6 and 8 hours. A Teflon coated internal fan ensured complete mixing of the chamber headspace volume. During the

35   experiments the chamber was kept at constant temperature (25°C, the mean daytime air temperature during

36   CYPHEX) and in darkness to avoid photochemical reactions. At the chamber outlet the emitted gases HONO, NO

1   and water vapor were quantified. HONO was analyzed with a commercial long path absorption photometer (LOPAP,

2   QUMA GmbH; Wuppertal, Germany), with a detection limit of ~4 ppt and 10% uncertainty (based on the

3   uncertainties of liquid and gas flow, concentration of calibration standard and regression of calibration). To avoid

4   any transformation of HONO in the tubing, the sampling unit including the stripping coil from LOPAP was directly

5   connected to the chamber. $NO_x$ (NO + $NO_2$) was detected with a commercial chemiluminescence detector (42i TL,

6   Thermo Scientific; Watham, USA) modified with a photolytic converter with a detection limit of ~50 ppt (NO) and

7   ~200 ppt ($NO_2$). An infrared $CO_2$ and $H_2O$ analyzer (Li-840A, LICOR; Lincoln, USA) was used to log the drying

8   and to calculate the soil water content (SWC) of the samples as follows:

9   $$SWC(WHC) = \frac{m_{H2O,t=n}}{m_{H2O,0}} * 100 \tag{eq. 3}$$

10   $$m_{H2O,t=n} = m_{H2O,t=n-1} - \frac{S_{Licor,t=n}}{\sum_{t=0}^{t=N} S_{Licor}} * m_{H2O,0} \tag{eq. 4}$$

11   with t=0 denoting the measurement start (wetted sample inserted into chamber), t=n: any time between 0 and N, t=N:

12   time when sample had dried out and measurement was stopped, $S_{Licor}$: absolute $H_2O$ signal at a given time, $m_{H2O,0}$:

13   mass of water added to sample (water holding capacity, WHC), SWC: soil water content in % WHC.

14   **2.5 Data analysis**

15   Measured data of $NO_2^-$, $NO_3^-$, $NH_4^+$, $Chl_{a+b}$, $Chl_a$, NO and HONO optimum flux and NO and HONO integrated flux

16   did not follow a normal distribution. Rather, log-transformed data were normally distributed (Shapiro-Wilk) and

17   therefore used for statistical analysis (Pearson correlation, ANOVA including Tukey Test with significance level of p

18   = 0.05) executed with OriginPro (version 9.0; OriginLab coporation, Northampton, Massachusetts, USA).

19   Precipitation data from the last 4 years (2013-2016) provided by the Department of Meteorology of Cyprus indicate

20   about 30 rain events per year (precipitation > 1 mm with following one or more dry days) were used to estimate

21   annual emissions of total nitrogen by way of HONO and NO.

22   **3 Results and discussion**

23   **3.1 Meteorological conditions**

24   One month before sampling, three sensors measuring temperature and relative humidity directly above the soil

25   surface were installed in the field to represent the micro-climate of the ground surface. Reference air temperature,

26   humidity and precipitation measurements at Paphos airport and Prodromos showed one rain event on 11-12 April

27   which is reflected by higher soil humidity (80-100%) and lower temperatures on these days (see Fig. 2). As a

28   consequence, the biological soil crusts were activated and went through one full wetting and drying cycle before

29   sample collection. Temperature above the soil ranged from 10°C in the night to 50°C during the day when solar

30   radiation was most intense. Air temperature was similar during the night but not as hot during the day ranging

31   between 20° and 30°C. Humidity above the ground was low during daytime (<30% rH) and increased during the

32   night up to 80%, while the atmospheric relative humidity (at Paphos airport) ranged between 47 and 73% (without

33   rain event). Thus there were only little variations of humidity with height above the soil surface. Above the ground

34   surface the relative humidity was somewhat lower during the day (mainly caused by higher temperatures) but

1     somewhat higher during the night, compared to respective weather station data. During and shortly after the main

2     rain event humidity at ground level was higher (80 and 100% rH) compared to ambient air humidity (70-85% rH).

3     Ambient air temperatures were somewhat lower during sample collection of this study as compared to the CYPHEX

4     field campaign in 2014. During CYPHEX, nighttime temperatures (3 m above ground level) did not drop below

5     18°C. Relative humidity (3 m above ground level) was mostly between 70 and 100% with only two short periods

6     with humidity between 20-60% rH. Hence we can assume that soil surface temperatures were higher and ground rH

7     in the same range during CYPHEX compared to sampling period.

8     **3.2 Cyprus soil and biocrust characteristics**

9     Systematic mapping of surface covers revealed that moss-dominated biocrusts are the most frequent in the

10    investigated Cyprus field site area (21.3%), followed by light (10.4%) and dark BSC (6.5%), whereas chlorolichen-

11    (3.2%) and cyanolichen-dominated BSC (1.8%) only played a minor role (Fig. 3, Fig. S1). The soil surface was

12    partially covered by litter (26.3%), stones (19.5%) and vascular vegetation (8.5%), whereas open soil was rarely

13    found (2.5%). It was previously established that soil and biocrusts emit HONO and NO (Weber et al., 2015; Oswald

14    et al., 2013), jointly accounting for 45.6% of surface area in our studied region. To the best of our knowledge, no

15    data on reactive nitrogen emissions from vascular vegetation and plant litter have been published yet.

16    Nutrient analysis revealed large variations in concentrations of nitrogen species ranging from 0 to 6.48, 0 to 0.57 and

17    0 to 22.2 mg (N) kg$^{-1}$ of dry soil/crust mass for $NO_3^-$, $NO_2^-$, and $NH_4^+$, respectively (Fig. 4a, Tab. S1 of the

18    supplement). In general, no significant change in reactive nitrogen contents was found before and after the trace gas

19    exchange experiments (Fig. 4a), indicating no significant impact of one wetting-drying cycle on the nutrient content.

20    Bare soil samples had significantly higher levels of $NO_3^-$ and $NO_2^-$ content compared to dark, chlorolichen and moss

21    BSC. Among the latter three, no significant differences in nutrient levels were observed. Light BSC had $NO_2^-$

22    contents similar to bare soil. The $NH_4^+$ content was very similar in all samples, except for one outlier in the group of

23    light BSC with strongly elevated $NH_4^+$. Higher nitrate and ammonium levels in bare soil compared to crust-covered

24    samples were also reported recently for a warm desert site in South Africa (Weber et al., 2015), indicative of nutrient

25    consumption/integration by the biocrusts. Nitrite, on the other hand, was lower for bare soil samples compared to

26    biocrust samples. While $NO_3^-$ was slightly higher, $NH_4^+$ and $NO_2^-$ contents (especially of bare soil samples) were

27    lower in the South African arid ecosystem compared to Cyprus.

28    Chlorophyll was only determined in the samples used for flux measurements. $Chl_a$ ranged from 4.1 (bare soil) to

29    144.2 mg m$^{-2}$ (moss BSC) and $Chl_{a+b}$ from 9.3 (bare soil) to 211.3 mg m$^{-2}$ (moss BSC), respectively (Fig. 4b, Tab.

30    S1). From bare soil, via light BSC and chlorolichen BSC II, to dark BSC the chlorophyll content increased, but not

31    significantly (p > 0.2). Nevertheless, $Chl_a$ and $Chl_{a+b}$ contents of chlorolichen BSC I and moss BSC were

32    significantly higher than these of bare soil, light BSC and chlorolichen BSC II (p<0.05, Fig. 4b).. The range of

33    chlorophyll contents is comparable to previous arid ecosystem studies (Weber et al., 2015).

34    The pH of soil and biocrusts ranged between slightly acidic (6.2) and slightly alkaline (7.6; Fig. 4c). The mean pH of

35    17 samples was 7.0, i.e., neutral. Only the pH of moss BSC samples was significantly lower than that of bare soil,

36    light BSC and chlorolichen BSC samples (p=0.05). Soil and biocrust samples from South Africa were slightly more

37    alkaline (7.1-8.2) with no significant difference among biocrust types (Weber et al., 2015).

Atmospheric
Chemistry
and Physics
Discussions

1 **3.3 NO and HONO flux measurements**

2 All samples showed HONO and NO emissions during full wetting and drying cycles. Maximum emission rates of

3 HONO were observed at about 17-33% WHC, and of NO at 20-36% with no significant differences between all soil

4 cover types (Fig 5). Emissions declined to zero at 0% WHC and to very small rates >70%. Emission maxima

5 strongly varied between soil cover types, but also between samples of the same cover type (see Fig. 5 and 6, and

6 Table S1). Highest emissions of both HONO-N and NO-N were detected for bare soil ($175 \pm 87.3$ and $92.2 \pm 34.7$ ng

7 $m^{-2} s^{-1}$), followed by light ($48.6 \pm 48.5$ and $34.5 \pm 42.1$ ng $m^{-2} s^{-1}$) and dark BSC ($27.1 \pm 35.9$ and $16.7 \pm 18.3$ ng $m^{-2}$

8 $s^{-1}$). Both types of chlorolichen- and moss-dominated biocrusts showed very low emission rates of reactive nitrogen

9 (on average < 10 ng $m^{-2} s^{-1}$). Maximum HONO emissions were somewhat higher than maximum NO emissions,

10 especially for bare soil. Integrating full wetting and drying cycles (6-8 hours), 0.04-1.9 mg $m^{-2}$ HONO-N and 0.06-

11 1.6 mg $m^{-2}$ NO-N were released (Fig. 6, lower panel). While the maximum fluxes of reactive nitrogen emission were

12 higher for HONO than NO, especially from bare soil, the integrated emissions were similar or even larger for NO,

13 which is released over a wider range of SWC.

14 In general, it is difficult to compare chamber flux measurements of different studies due to different experimental

15 configurations, such as chamber dimension, flow rate, resident time and drying rate etc. Here, we compare our

16 results to studies which applied the same method (with the same or very similar conditions). The emission rates are

17 consistent with these studies where HONO-N or NO-N emissions from soil between 1-3000 ng $m^{-2} s^{-1}$ were found

18 (Su et al., 2011; Oswald et al., 2013; Mamtimin et al., 2016; Wu et al., 2014; Weber et al., 2015). Mamtimin et al.

19 (2016) observed NO-N fluxes at 25°C of 57.5 ng $m^{-2} s^{-1}$, 18.9 ng $m^{-2} s^{-1}$ and 4.1 ng $m^{-2} s^{-1}$ for soil of grape and cotton

20 fields and desert soil from an oasis in China, respectively. Oswald et al. (2013) found HONO-N and NO-N emissions

21 between 2 and 280 ng $m^{-2} s^{-1}$ (each) from different soil from all over the world covering a wide range of pH, nutrient

22 content and organic matter. Biogenic NO emissions of 44 soil samples from arid and semi-arid regions were

23 reviewed by Meixner and Yang (2006) with N-fluxes ranging from 0 to 142 ng $m^{-2} s^{-1}$.

24 In contrast to the results of the present study, where bare soil showed highest emissions, Weber et al. (2015) found

25 lowest emission from bare soil in samples from South Africa. In that study, dark cyanobacteria-dominated biocrusts

26 revealed highest emission rates (each HONO-N and NO-N up to 200 ng $m^{-2} s^{-1}$), followed by light cyanobacteria-

27 dominated biocrusts (up to 120 ng $m^{-2} s^{-1}$), whereas in the present study, emissions of dark cyanobacteria-dominated

28 biocrusts tended to be lower. No significant difference of HONO-N and NO-N emissions from light BSC between

29 both sample origins were found. HONO-N and NO-N emissions of moss- and chlorolichen-dominated biocrusts were

30 low in both studies (each <60 ng $m^{-2} s^{-1}$) but still significantly higher for samples from South Africa than from

31 Cyprus. In the present study HONO maximum emissions were higher than for NO (while integrated emissions being

32 comparable) while in the study of Weber et al. (2015) HONO maximum fluxes were somewhat lower than those of

33 NO. The present results of nitrogen emissions correlate well with the nutrient contents (especially $NO_2^-$ and $NO_3^-$,

34 Fig. 7). Bare soil, in which highest $NO_3^-$ and $NO_2^-$ levels were found, also showed highest HONO and NO emissions.

35 A very good correlation was found between $NO_2^-$ contents and emission of both nitrogen gas phase species for all

36 samples ($R^2 = 0.84$ for HONO and 0.85 for NO; $p<0.001$). The level of correlation between $NO_3^-$ and HONO and

37 NO was lower, but still significant ($R^2 = 0.68$ and 0.67, respectively, $p<0.001$). Only low correlations were found

38 between HONO or NO emissions and $NH_4^+$-contents ($R^2 = 0.165$ and 0.232; $p=0.05$). Thus, in the present study it

1   seems that reactive nitrogen emissions predominantly depend on $NO_2^-$ and $NO_3^-$ contents and not on surface cover

2   types, although biocrusts (especially with cyanobacteria and cyanolichens) are able to fix atmospheric nitrogen

3   (Belnap, 2002; Elbert et al., 2012; Barger et al., 2013; Patova et al., 2016). The results of a two-factorial ANOVA

4   showed that HONO or NO emissions are not significantly related to soil cover type but rather with nitrite content,

5   i.e., its direct aqueous precursor. For nitrate, the two-factorial ANOVA indicated dependencies of both cover type

6   and nutrient content. These results differ from those obtained by Weber et al. (2015) on South African samples, as

7   there HONO and NO emissions were not correlated with bulk concentrations of ammonium, nitrite and nitrate. In

8   their study nitrite content was lowest for bare soil compared to other biocrust types. Ammonium and nitrites levels

9   were also lower than in the present study. Therefore Weber et al. (2015) indicated that biocrusts can enhance N-cycle

10  and emission of reactive nitrogen.

11  **3.4 Comparison of soil emission and observed missing source**

12  To quantify the flux rate of HONO emissions from soil to the local atmosphere and to compare it to the unaccounted

13  source found in Cyprus in 2014 (Meusel et al., 2016), we applied a standard formalism describing the atmosphere-

14  soil exchange of trace gases as a function of the difference between the atmospheric concentration and the

15  equilibrium concentration at the soil solution surface [HONO]* (Su et al., 2011):

16  $$F^* = v_T \; ([HONO]^* - [HONO]) \qquad (eq.5)$$

17  where [HONO] is the ambient HONO concentration measured on Cyprus (mean daytime average 60 ppt) and

18  [HONO]* is the equilibrium concentration at soil surface. [HONO]* can be determined from measurements in a

19  static chamber. In a dynamic chamber system, there is a concentration gradient of HONO between the headspace

20  (where HONO was measured) and the soil surface. Here we use the measurements of water vapor to correct for the

21  soil surface concentration and equilibrium concentration of HONO by assuming a similar gradient for the two

22  species. A correction coefficient of 3.8 was determined, which is the ratio of the equilibrium rH of 100% over wet

23  soil surface to the initial headspace rH of 25-30% after inserting the wet sample into the chamber. The transfer

24  velocity, $v_t$, depends primarily on meteorological and soil conditions, and is typically on the order of ~1 cm s$^{-1}$. The

25  flux rate of NO was calculated accordingly with mean daytime NO concentrations of 38 ppt. The calculated flux F*

26  is about (67±3) % of the flux measured in the chamber.

27  The distribution of nine different surface cover types was mapped (Fig. 2), including stones, vascular vegetation and

28  litter not being attributed to emit significant amounts of HONO and NO to the atmosphere. The residual HONO

29  emitting surface covers comprised 45.6% of total surface in the investigated area. Combining the information on

30  soil/biocrust population and the calculated flux F*, a site-specific community emission $F_{comm}$ of HONO and NO can

31  be estimated via following equation (eq. 6).

32  $$F_{comm,max} = \sum_i^{type} F_{max,i}^* * p_i/100 \qquad or \qquad F_{comm,int} = \sum_i^{type} F_{int,i}^* * p_i/100 \qquad (eq. 6)$$

33  where $F_{comm}$ denotes the estimated community flux, $F_{max,i \; or \; int,i}^*$ the maximum or integrated emission rates of each

34  individual surface cover type i [ng N m$^{-2}$ s$^{-1}$ or µg N m$^{-2}$] and $p_i$ the fraction of population type i [%].

35  Under optimum soil water conditions (20-30% WHC) and constant temperatures of about 25°C, between 2.2 and

36  18.8 ng m$^{-2}$ s$^{-1}$ of total HONO-N and 1.6-16.2 ng m$^{-2}$ s$^{-1}$ of total NO-N are emitted from the different crust/soil

37  population combinations derived from the vegetation cover assessment. In the lower range of total emissions the

1    contribution from bare soil dominated with up to 69% (HONO) and 55% (NO), respectively, followed by moss BSC

2    (HONO: 23%; NO: 32%). At high levels of total emission, the contribution from light BSC dominated (HONO:

3    43%, NO: 49%), decreasing the contribution of bare soil down to about 25% (HONO) and 13% (NO). Emissions

4    from dark BSC contribute about 20% or 24% to the total HONO or NO flux while the contribution from moss BSC

5    decreased to 10% or 12%, respectively. Emissions from chlorolichen BSC didn´t play a significant role (< 2.4%) in

6    general (see Fig. 8).

7    After heavy rainfalls moistening the soil to full water-holding capacity, 11-113 µg m$^{-2}$ of HONO-N and 10-131 µg

8    m$^{-2}$ of NO-N can be calculated for one complete wetting-and-drying period. Assuming 30 rain events per year (based

9    on the statistic of 4 years precipitation data), a wetting-drying cycle time of 7 days, and constant emissions in

10    between them (at 10% WHC) up to 160 mg m$^{-2}$ yr$^{-1}$ of nitrogen can be emitted directly by the sum of HONO-N and

11    NO-N from Cyprus natural ground surfaces, i.e., excluding heterogeneous conversion of $NO_2$ on ground surface.

12    The release of HONO from the ground surface to the atmosphere can be related to the atmospheric HONO

13    production rate via eq. 7 (adapted from Su et al., 2011) and then compared to the missing source.

14               $S_{ground} = \frac{0.35 * F_{comm,max}}{BLH} * a$                       (eq.7)

15    with $S_{ground}$: HONO or NO emitted from ground surface; BLH: boundary layer height (mixed layer height) and a:

16    factor to convert ng N in number of molecules ($10^{-9} * 6.022 \times 10^{23}/14$).

17    Based on the studies by Likos (2008) and Leelamanie (2010) and the meteorological conditions during CYPHEX (no

18    rain event, but high rH, usually > 75%) a soil water content, slightly lower than the optimal water content for HONO

19    and NO emissions, of 10% WHC was estimated, at which emissions of about 35% of the maximum was found.

20    In Cyprus during the summer of 2014 a mean boundary layer height of 300 m was observed by means of a

21    ceilometer.. The mean air temperature during the campaign was comparable to the lab based chamber studies (25°C)

22    but soil temperatures at the Cyprus field site could largely vary during daytime and reach maximum temperatures of

23    up to 50°C (Fig. 4). At these high temperatures 6-10 fold higher emissions can be expected in general (Mamtimin et

24    al., 2016), but also a quicker drying of the soil and biocrusts. At 25°C HONO emissions from the ground would

25    equal a source strength of $1.1 \times 10^5$-$9.8 \times 10^5$ cm$^{-3}$ s$^{-1}$ and would cover up to 75% of the missing mean source of $1.3 \times 10^6$

26    cm$^{-3}$ s$^{-1}$ (Meusel et al., 2016). In some mornings of the campaign dew formation was expected causing an increase in

27    soil humidity. Combined with rising temperatures after sun-rise these optimized meteorological conditions may have

28    led to enhanced soil emissions and would confer a reasonable explanation for the strong HONO morning peaks

29    observed during the campaign. Similarly, the NO source strength from ground emission at 25°C is in the range from

30    $8.3 \times 10^4$ to $8.0 \times 10^5$ cm$^{-3}$ s$^{-1}$. As the observed unaccounted source of NO in Cyprus was of the order of $10^7$ cm$^{-3}$ s$^{-1}$ soil

31    emissions can only contribute up to 8% indicating other NO sources. Note that during CYPHEX there were two

32    periods with lower rH, in which even a NO sink was detected.

33    **4 Conclusions**

34    HONO and NO emission rates from soil and biological soil crusts were derived by means of lab-based enclosure

35    trace gas exchange measurements, and revealed quite similar ranges of reactive nitrogen source strengths. Emissions

36    of both compounds strongly correlated with $NO_2^-$ and $NO_3^-$ content of the samples. Emissions from bare soil were

Atmospheric
Chemistry
and Physics
Discussions

1   highest, but bare soil surface spots were rarely found at the investigated CYPHEX field study site. The estimated

2   total ground surface HONO flux in the natural habitat is consistent with the previously unaccounted source estimated

3   for Cyprus, i.e., the unaccounted HONO source can essentially be explained by emissions from soil/biocrusts. For

4   NO, the measured and simulated fluxes cannot account for the unaccounted NO source (during the humid periods of

5   the CYPHEX campaign 2014), indicating that emission from soil was not the only missing source of NO.

6   **References**

7   Abed, R. M. M., Lam, P., de Beer, D., and Stief, P.: High rates of denitrification and nitrous oxide emission in arid

8      biological soil crusts from the Sultanate of Oman, Isme Journal, 7, 1862-1875, 10.1038/ismej.2013.55, 2013.

9   Alicke, B., Platt, U., and Stutz, J.: Impact of nitrous acid photolysis on the total hydroxyl radical budget during the

10     Limitation of Oxidant Production/Pianura Padana Produzione di Ozono study in Milan, Journal of Geophysical

11     Research-Atmospheres, 107, 10.1029/2000jd000075, 2002.

12   Ammann, M., Kalberer, M., Jost, D. T., Tobler, L., Rossler, E., Piguet, D., Gaggeler, H. W., and Baltensperger, U.:

13     Heterogeneous production of nitrous acid on soot in polluted air masses, Nature, 395, 157-160, 10.1038/25965,

14     1998.

15   Arens, F., Gutzwiller, L., Baltensperger, U., Gaggeler, H. W., and Ammann, M.: Heterogeneous reaction of NO2 on

16     diesel soot particles, Environmental Science & Technology, 35, 2191-2199, 10.1021/es000207s, 2001.

17   Aubin, D. G., and Abbatt, J. P. D.: Interaction of $NO_2$ with hydrocarbon soot: Focus on HONO yield, surface

18     modification, and mechanism, Journal of Physical Chemistry A, 111, 6263-6273, 10.1021/jp068884h, 2007.

19   Baergen, A. M., and Donaldson, D. J.: Photochemical renoxification of nitric acid on real urban grime,

20     Environmental Science & Technology, 47, 815-820, 10.1021/es3037862, 2013.

21   Barger, N. N., Castle, S. C., and Dean, G. N.: Denitrification from nitrogen-fixing biologically crusted soils in a cool

22     desert environment, southeast Utah, USA, Ecological Processes, 2, 16, 10.1186/2192-1709-2-16, 2013.

23   Barger, N. N., Weber, B., Garcia-Pichel, F., Zaady, E., Belnap, J.: Patterns and controls on nitrogen cycling of

24     biological soil crusts. In: Weber, B., Büdel, B., Belnap, J. (eds) Biological soil crusts: An organizing principle in

25     drylands, Ecological Studies 226, Springer International Publishing Switzerland, pp 257-285, 2016.

26   Bejan, I., Abd El Aal, Y., Barnes, I., Benter, T., Bohn, B., Wiesen, P., and Kleffmann, J.: The photolysis of ortho-

27     nitrophenols: a new gas phase source of HONO, Physical Chemistry Chemical Physics, 8, 2028-2035,

28     10.1039/b516590c, 2006.

29   Belnap, J.: Nitrogen fixation in biological soil crusts from southeast Utah, USA, Biology and Fertility of Soils, 35,

30     128-135, 10.1007/s00374-002-0452-x, 2002.

31   Belnap, J., Weber, B., Büdel, B.: Biological soil crusts as an organizing principle in drylands. In: Weber, B., Büdel,

32     B., Belnap, J. (eds) Biological soil crusts: An organizing principle in drylands, Ecological Studies 226, Springer

33     International Publishing Switzerland, pp 3-13, 2016.

34   Broske, R., Kleffmann, J., and Wiesen, P.: Heterogeneous conversion of $NO_2$ on secondary organic aerosol surfaces:

35     A possible source of nitrous acid (HONO) in the atmosphere?, Atmospheric Chemistry and Physics, 3, 469-474,

36     2003.

Atmospheric
Chemistry
and Physics
Discussions

1    Büdel, B., Darienko, T., Deutschewitz, K., Dojani, S., Friedl, T., Mohr, K., Salisch, M., Reisser, W. and Weber, B.:
2        Southern African biological soil crusts are ubiquitous and highly diverse in drylands, being restricted by rainfall
3        frequency. Microbial Ecology 57(2): 229-47, 2009.
4    Cleveland, C. C., Townsend, A. R., Schimel, D. S., Fisher, H., Howarth, R. W., Hedin, L. O., Perakis, S. S., Latty, E.
5        F., Von Fischer, J. C., Elseroad, A., and Wasson, M. F.: Global patterns of terrestrial biological nitrogen ($N_2$)
6        fixation in natural ecosystems, Global Biogeochemical Cycles, 13, 623-645, 10.1029/1999gb900014, 1999.
7    Czader, B. H., Rappenglueck, B., Percell, P., Byun, D. W., Ngan, F., and Kim, S.: Modeling nitrous acid and its
8        impact on ozone and hydroxyl radical during the Texas Air Quality Study 2006, Atmospheric Chemistry and
9        Physics, 12, 6939-6951, 10.5194/acp-12-6939-2012, 2012.
10   Darby, B. J., Neher, D. A.: Microfauna within biological soil crusts. In: Weber, B., Büdel, B., Belnap, J. (eds)
11       Biological soil crusts: An organizing principle in drylands, Ecological Studies 226, Springer International
12       Publishing Switzerland, pp 139-157, 2016.
13   Dumack, K., Koller, R., Weber, B. and Bonkowski, M.: Estimated heterotrophic protist abundances and their
14       diversity in South African biological soil crusts. South African Journal of Science 112(7/8). Art. #2015-0302, 5
15       pages. http://dx.doi.org/10.17159/sajs.2016/20150302, 2016
16   Elbert, W., Weber, B., Burrows, S., Steinkamp, J., Budel, B., Andreae, M. O., and Poschl, U.: Contribution of
17       cryptogamic covers to the global cycles of carbon and nitrogen, Nature Geosci, 5, 459-462,
18       http://www.nature.com/ngeo/journal/v5/n7/abs/ngeo1486.html#supplementary-information, 2012.
19   George, C., Strekowski, R. S., Kleffmann, J., Stemmler, K., and Ammann, M.: Photoenhanced uptake of gaseous
20       $NO_2$ on solid-organic compounds: a photochemical source of HONO?, Faraday Discussions, 130, 195-210,
21       10.1039/b417888m, 2005.
22   Han, C., Yang, W. J., Wu, Q. Q., Yang, H., and Xue, X. X.: Heterogeneous photochemical conversion of $NO_2$ to
23       HONO on the humic acid surface under simulated sunlight, Environmental Science & Technology, 50, 5017-
24       5023, 10.1021/acs.est.5b05101, 2016.
25   Harrison, R. M., and Kitto, A. M. N.: Evidence for a surface source of atmospheric nitrous acid, Atmospheric
26       Environment, 28, 1089-1094, 10.1016/1352-2310(94)90286-0, 1994.
27   Herridge, D. F., Peoples, M. B., and Boddey, R. M.: Global inputs of biological nitrogen fixation in agricultural
28       systems, Plant and Soil, 311, 1-18, 10.1007/s11104-008-9668-3, 2008.
29   Johnson, S. L., Budinoff, C. R., Belnap, J., and Garcia-Pichel, F.: Relevance of ammonium oxidation within
30       biological soil crust communities, Environmental Microbiology, 7, 1-12, 10.1111/j.1462-2920.2004.00649.x,
31       2005.
32   Kalberer, M., Ammann, M., Arens, F., Gaggeler, H. W., and Baltensperger, U.: Heterogeneous formation of nitrous
33       acid (HONO) on soot aerosol particles, Journal of Geophysical Research-Atmospheres, 104, 13825-13832,
34       10.1029/1999jd900141, 1999.
35   Kebede, M. A., Scharko, N. K., Appelt, L. E., and Raff, J. D.: Formation of nitrous acid during ammonia
36       photooxidation on $TiO_2$ under atmospherically relevant conditions, Journal of Physical Chemistry Letters, 4,
37       2618-2623, 10.1021/jz401250k, 2013.

Atmospheric
Chemistry
and Physics
Discussions

1   Kinugawa, T., Enami, S., Yabushita, A., Kawasaki, M., Hoffmann, M. R., and Colussi, A. J.: Conversion of gaseous
2      nitrogen dioxide to nitrate and nitrite on aqueous surfactants, Physical Chemistry Chemical Physics, 13, 5144-
3      5149, 10.1039/C0CP01497D, 2011.
4   Kleffmann, J., H. Becker, K., Lackhoff, M., and Wiesen, P.: Heterogeneous conversion of $NO_2$ on carbonaceous
5      surfaces, Physical Chemistry Chemical Physics, 1, 5443-5450, 10.1039/A905545B, 1999.
6   Kleffmann, J., Kurtenbach, R., Lorzer, J., Wiesen, P., Kalthoff, N., Vogel, B., and Vogel, H.: Measured and
7      simulated vertical profiles of nitrous acid - Part I: Field measurements, Atmospheric Environment, 37, 2949-
8      2955, 10.1016/s1352-2310(03)00242-5, 2003.
9   Kleffmann, J., Gavriloaiei, T., Hofzumahaus, A., Holland, F., Koppmann, R., Rupp, L., Schlosser, E., Siese, M., and
10      Wahner, A.: Daytime formation of nitrous acid: A major source of OH radicals in a forest, Geophysical Research
11      Letters, 32, 10.1029/2005gl022524, 2005.
12  Kleffmann, J., and Wiesen, P.: Heterogeneous conversion of $NO_2$ and NO on $HNO_3$ treated soot surfaces:
13      atmospheric implications, Atmospheric Chemistry and Physics, 5, 77-83, 2005.
14  Langridge, J. M., Gustafsson, R. J., Griffiths, P. T., Cox, R. A., Lambert, R. M., and Jones, R. L.: Solar driven
15      nitrous acid formation on building material surfaces containing titanium dioxide: A concern for air quality in
16      urban areas?, Atmospheric Environment, 43, 5128-5131, http://dx.doi.org/10.1016/j.atmosenv.2009.06.046,
17      2009.
18  Lelièvre, S., Bedjanian, Y., Laverdet, G., and Le Bras, G.: Heterogeneous reaction of $NO_2$ with hydrocarbon flame
19      soot, The Journal of Physical Chemistry A, 108, 10807-10817, 10.1021/jp0469970, 2004.
20  Li, X., Rohrer, F., Hofzumahaus, A., Brauers, T., Häseler, R., Bohn, B., Broch, S., Fuchs, H., Gomm, S., Holland, F.,
21      Jäger, J., Kaiser, J., Keutsch, F. N., Lohse, I., Lu, K., Tillmann, R., Wegener, R., Wolfe, G. M., Mentel, T. F.,
22      Kiendler-Scharr, A., and Wahner, A.: Missing gas-phase source of HONO inferred from Zeppelin measurements
23      in the troposphere, Science, 344, 292-296, 10.1126/science.1248999, 2014.
24  Liu, Y., Han, C., Ma, J., Bao, X., and He, H.: Influence of relative humidity on heterogeneous kinetics of $NO_2$ on
25      kaolin and hematite, Physical Chemistry Chemical Physics, 17, 19424-19431, 10.1039/c5cp02223a, 2015.
26  Mamtimin, B., Meixner, F. X., Behrendt, T., Badawy, M., and Wagner, T.: The contribution of soil biogenic NO and
27      HONO emissions from a managed hyperarid ecosystem to the regional NOx emissions during growing season,
28      Atmos. Chem. Phys., 16, 10175-10194, 10.5194/acp-16-10175-2016, 2016.
29  Meixner, F. X., and Yang, W. X.: Biogenic emissions of nitric oxide and nitrous oxide from arid and semi-arid land,
30      in: Dryland Ecohydrology, edited by: D'Odorico, P., and Porporato, A., Springer Netherlands, Dordrecht, 233-
31      255, 2006.
32  Meusel, H., Kuhn, U., Reiffs, A., Mallik, C., Harder, H., Martinez, M., Schuladen, J., Bohn, B., Parchatka, U.,
33      Crowley, J. N., Fischer, H., Tomsche, L., Novelli, A., Hoffmann, T., Janssen, R. H. H., Hartogensis, O., Pikridas,
34      M., Vrekoussis, M., Bourtsoukidis, E., Weber, B., Lelieveld, J., Williams, J., Pöschl, U., Cheng, Y., and Su, H.:
35      Daytime formation of nitrous acid at a coastal remote site in Cyprus indicating a common ground source of
36      atmospheric HONO and NO, Atmos. Chem. Phys., 16, 14475-14493, 10.5194/acp-16-14475-2016, 2016.

Atmospheric
Chemistry
and Physics
Discussions

1    Meusel, H., Elshorbany, Y., Kuhn, U., Bartels-Rausch, T., Reinmuth-Selzle, K., Kampf, C. J., Li, G., Wang, X.,
2      Lelieveld, J., Pöschl, U., Hoffmann, T., Su, H., Ammann, M., and Cheng, Y.: Light-induced protein nitration and
3      degradation with HONO emission, Atmos. Chem. Phys. Discuss., 2017, 1-22, 10.5194/acp-2017-277, 2017.

4    Michoud, V., Colomb, A., Borbon, A., Miet, K., Beekmann, M., Camredon, M., Aumont, B., Perrier, S., Zapf, P.,
5      Siour, G., Ait-Helal, W., Afif, C., Kukui, A., Furger, M., Dupont, J. C., Haeffelin, M., and Doussin, J. F.: Study
6      of the unknown HONO daytime source at a European suburban site during the MEGAPOLI summer and winter
7      field campaigns, Atmospheric Chemistry and Physics, 14, 2805-2822, 10.5194/acp-14-2805-2014, 2014.

8    Monge, M. E., D'Anna, B., Mazri, L., Giroir-Fendler, A., Ammann, M., Donaldson, D. J., and George, C.: Light
9      changes the atmospheric reactivity of soot, Proceedings of the National Academy of Sciences of the United States
10     of America, 107, 6605-6609, 10.1073/pnas.0908341107, 2010.

11    Ndour, M., D'Anna, B., George, C., Ka, O., Balkanski, Y., Kleffmann, J., Stemmler, K., and Ammann, M.:
12     Photoenhanced uptake of $NO_2$ on mineral dust: Laboratory experiments and model simulations, Geophysical
13     Research Letters, 35, 10.1029/2007gl032006, 2008.

14    Neuman, J. A., Trainer, M., Brown, S. S., Min, K. E., Nowak, J. B., Parrish, D. D., Peischl, J., Pollack, I. B., Roberts,
15     J. M., Ryerson, T. B., and Veres, P. R.: HONO emission and production determined from airborne measurements
16     over the Southeast U.S, Journal of Geophysical Research: Atmospheres, 121, 9237-9250,
17     10.1002/2016JD025197, 2016.

18    Oswald, R., Behrendt, T., Ermel, M., Wu, D., Su, H., Cheng, Y., Breuninger, C., Moravek, A., Mougin, E., Delon,
19     C., Loubet, B., Pommerening-Roeser, A., Soergel, M., Poeschl, U., Hoffmann, T., Andreae, M. O., Meixner, F.
20     X., and Trebs, I.: HONO emissions from soil bacteria as a major source of atmospheric reactive nitrogen,
21     Science, 341, 1233-1235, 10.1126/science.1242266, 2013.

22    Oswald, R., Ermel, M., Hens, K., Novelli, A., Ouwersloot, H. G., Paasonen, P., Petaja, T., Sipila, M., Keronen, P.,
23     Back, J., Konigstedt, R., Beygi, Z. H., Fischer, H., Bohn, B., Kubistin, D., Harder, H., Martinez, M., Williams, J.,
24     Hoffmann, T., Trebs, I., and Soergel, M.: A comparison of HONO budgets for two measurement heights at a field
25     station within the boreal forest in Finland, Atmospheric Chemistry and Physics, 15, 799-813, 10.5194/acp-15-
26     799-2015, 2015.

27    Patova, E., Sivkov, M., and Patova, A.: Nitrogen fixation activity in biological soil crusts dominated by
28     cyanobacteria in the Subpolar Urals (European North-East Russia), FEMS Microbiology Ecology, 92,
29     10.1093/femsec/fiw131, 2016.

30    Pilegaard, K.: Processes regulating nitric oxide emissions from soils, Philosophical Transactions of the Royal Society
31     B: Biological Sciences, 368, 10.1098/rstb.2013.0126, 2013.

32    Ramazan, K. A., Syomin, D., and Finlayson-Pitts, B. J.: The photochemical production of HONO during the
33     heterogeneous hydrolysis of $NO_2$, Physical Chemistry Chemical Physics, 6, 3836-3843, 10.1039/b402195a, 2004.

34    Ren, X. R., Harder, H., Martinez, M., Lesher, R. L., Oliger, A., Simpas, J. B., Brune, W. H., Schwab, J. J.,
35     Demerjian, K. L., He, Y., Zhou, X. L., and Gao, H. G.: OH and $HO_2$ chemistry in the urban atmosphere of New
36     York City, Atmospheric Environment, 37, 3639-3651, 10.1016/s1352-2310(03)00459-x, 2003.

37    Ren, X., Brune, W. H., Oliger, A., Metcalf, A. R., Simpas, J. B., Shirley, T., Schwab, J. J., Bai, C., Roychowdhury,
38     U., Li, Y., Cai, C., Demerjian, K. L., He, Y., Zhou, X., Gao, H., and Hou, J.: OH, $HO_2$, and OH reactivity during

1  the PMTACS-NY Whiteface Mountain 2002 campaign: Observations and model comparison, Journal of
2  Geophysical Research-Atmospheres, 111, 10.1029/2005jd006126, 2006.

3  Ren, X., Sanders, J. E., Rajendran, A., Weber, R. J., Goldstein, A. H., Pusede, S. E., Browne, E. C., Min, K. E., and
4  Cohen, R. C.: A relaxed eddy accumulation system for measuring vertical fluxes of nitrous acid, Atmospheric
5  Measurement Techniques, 4, 2093-2103, 10.5194/amt-4-2093-2011, 2011.

6  Ronen, R., and Galun, M.: Pigment extraction from lichens with dimethylsufoxide (DMSO) and estimation of
7  chlorophyll degradation, Environmental and Experimental Botany, 24, 239-245, 10.1016/0098-8472(84)90004-2,
8  1984.

9  Sarwar, G., Roselle, S. J., Mathur, R., Appel, W., Dennis, R. L., and Vogel, B.: A comparison of CMAQ HONO
10  predictions with observations from the Northeast Oxidant and Particle Study, Atmospheric Environment, 42,
11  5760-5770, http://dx.doi.org/10.1016/j.atmosenv.2007.12.065, 2008.

12  Scharko, N. K., Berke, A. E., and Raff, J. D.: Release of nitrous acid and nitrogen dioxide from nitrate photolysis in
13  acidic aqueous solutions, Environmental Science & Technology, 48, 11991-12001, 10.1021/es503088x, 2014.

14  Soergel, M., Regelin, E., Bozem, H., Diesch, J. M., Drewnick, F., Fischer, H., Harder, H., Held, A., Hosaynali-
15  Beygi, Z., Martinez, M., and Zetzsch, C.: Quantification of the unknown HONO daytime source and its relation
16  to NO2, Atmospheric Chemistry and Physics, 11, 10433-10447, 10.5194/acp-11-10433-2011, 2011a.

17  Stemmler, K., Ammann, M., Donders, C., Kleffmann, J., and George, C.: Photosensitized reduction of nitrogen
18  dioxide on humic acid as a source of nitrous acid, Nature, 440, 195-198, 10.1038/nature04603, 2006.

19  Stemmler, K., Ndour, M., Elshorbany, Y., Kleffmann, J., D'Anna, B., George, C., Bohn, B., and Ammann, M.: Light
20  induced conversion of nitrogen dioxide into nitrous acid on submicron humic acid aerosol, Atmospheric
21  Chemistry and Physics, 7, 4237-4248, 2007.

22  Strauss, S. L., Day, T. A., and Garcia-Pichel, F.: Nitrogen cycling in desert biological soil crusts across
23  biogeographic regions in the Southwestern United States, Biogeochemistry, 108, 171-182, 10.1007/s10533-011-
24  9587-x, 2012.

25  Stutz, J., Alicke, B., and Neftel, A.: Nitrous acid formation in the urban atmosphere: Gradient measurements of NO$_2$
26  and HONO over grass in Milan, Italy, Journal of Geophysical Research-Atmospheres, 107,
27  10.1029/2001jd000390, 2002.

28  Su, H., Cheng, Y. F., Cheng, P., Zhang, Y. H., Dong, S., Zeng, L. M., Wang, X., Slanina, J., Shao, M., and
29  Wiedensohler, A.: Observation of nighttime nitrous acid (HONO) formation at a non-urban site during PRIDE-
30  PRD2004 in China, Atmospheric Environment, 42, 6219-6232, 10.1016/j.atmosenv.2008.04.006, 2008a.

31  Su, H., Cheng, Y. F., Shao, M., Gao, D. F., Yu, Z. Y., Zeng, L. M., Slanina, J., Zhang, Y. H., and Wiedensohler, A.:
32  Nitrous acid (HONO) and its daytime sources at a rural site during the 2004 PRIDE-PRD experiment in China,
33  Journal of Geophysical Research-Atmospheres, 113, 10.1029/2007jd009060, 2008b.

34  Su, H., Cheng, Y., Oswald, R., Behrendt, T., Trebs, I., Meixner, F. X., Andreae, M. O., Cheng, P., Zhang, Y., and
35  Poeschl, U.: Soil nitrite as a source of atmospheric HONO and OH radicals, Science, 333, 1616-1618,
36  10.1126/science.1207687, 2011.

Atmospheric
Chemistry
and Physics
Discussions

Open Access

EGU

1  Tang, Y., An, J., Wang, F., Li, Y., Qu, Y., Chen, Y., and Lin, J.: Impacts of an unknown daytime HONO source on
2      the mixing ratio and budget of HONO, and hydroxyl, hydroperoxyl, and organic peroxy radicals, in the coastal
3      regions of China, Atmospheric Chemistry and Physics, 15, 9381-9398, 10.5194/acp-15-9381-2015, 2015.
4  VandenBoer, T. C., Brown, S. S., Murphy, J. G., Keene, W. C., Young, C. J., Pszenny, A. A. P., Kim, S., Warneke,
5      C., de Gouw, J. A., Maben, J. R., Wagner, N. L., Riedel, T. P., Thornton, J. A., Wolfe, D. E., Dubé, W. P.,
6      Öztürk, F., Brock, C. A., Grossberg, N., Lefer, B., Lerner, B., Middlebrook, A. M., and Roberts, J. M.:
7      Understanding the role of the ground surface in HONO vertical structure: High resolution vertical profiles during
8      NACHTT-11, Journal of Geophysical Research: Atmospheres, 118, 10,155-110,171, 10.1002/jgrd.50721, 2013.
9  Villena, G., Kleffmann, J., Kurtenbach, R., Wiesen, P., Lissi, E., Rubio, M. A., Croxatto, G., and Rappenglueck, B.:
10     Vertical gradients of HONO, NOx and O$_3$ in Santiago de Chile, Atmospheric Environment, 45, 3867-3873,
11     10.1016/j.atmosenv.2011.01.073, 2011.
12  Vogel, B., Vogel, H., Kleffmann, J., and Kurtenbach, R.: Measured and simulated vertical profiles of nitrous acid -
13     Part II. Model simulations and indications for a photolytic source, Atmospheric Environment, 37, 2957-2966,
14     10.1016/s1352-2310(03)00243-7, 2003.
15  Wang, S. H., Ackermann, R., Spicer, C. W., Fast, J. D., Schmeling, M., and Stutz, J.: Atmospheric observations of
16     enhanced NO$_2$-HONO conversion on mineral dust particles, Geophysical Research Letters, 30,
17     10.1029/2003gl017014, 2003.
18  Weber, B., Wessels, D. C., Deutschewitz, K., Dojani, S., Reichenberger, H., and Büdel, B.: Ecological
19     characterization of soil-inhabiting and hypolithic soil crusts within the Knersvlakte, South Africa, Ecological
20     Processes, 2, 8, 10.1186/2192-1709-2-8, 2013.
21  Weber, B., Wu, D., Tamm, A., Ruckteschler, N., Rodriguez-Caballero, E., Steinkamp, J., Meusel, H., Elbert, W.,
22     Behrendt, T., Soergel, M., Cheng, Y., Crutzen, P. J., Su, H., and Poeschl, U.: Biological soil crusts accelerate the
23     nitrogen cycle through large NO and HONO emissions in drylands, Proceedings of the National Academy of
24     Sciences of the United States of America, 112, 15384-15389, 10.1073/pnas.1515818112, 2015.
25  Wong, K. W., Tsai, C., Lefer, B., Haman, C., Grossberg, N., Brune, W. H., Ren, X., Luke, W., and Stutz, J.: Daytime
26     HONO vertical gradients during SHARP 2009 in Houston, TX, Atmospheric Chemistry and Physics, 12, 635-
27     652, 10.5194/acp-12-635-2012, 2012.
28  Wong, K. W., Tsai, C., Lefer, B., Grossberg, N., and Stutz, J.: Modeling of daytime HONO vertical gradients during
29     SHARP 2009, Atmospheric Chemistry and Physics, 13, 3587-3601, 10.5194/acp-13-3587-2013, 2013.
30  Wu, D., Kampf, C. J., Pöschl, U., Oswald, R., Cui, J., Ermel, M., Hu, C., Trebs, I., and Sörgel, M.: Novel tracer
31     method to measure isotopic labeled gas-phase nitrous acid (HO$^{15}$NO) in Biogeochemical Studies, Environmental
32     Science & Technology, 48, 8021-8027, 10.1021/es501353x, 2014.
33  Yabushita, A., Enami, S., Sakamoto, Y., Kawasaki, M., Hoffmann, M. R., and Colussi, A. J.: Anion-catalyzed
34     dissolution of NO$_2$ on aqueous microdroplets, The Journal of Physical Chemistry A, 113, 4844-4848,
35     10.1021/jp900685f, 2009.
36  Young, C. J., Washenfelder, R. A., Roberts, J. M., Mielke, L. H., Osthoff, H. D., Tsai, C., Pikelnaya, O., Stutz, J.,
37     Veres, P. R., Cochran, A. K., VandenBoer, T. C., Flynn, J., Grossberg, N., Haman, C. L., Lefer, B., Stark, H.,
38     Graus, M., de Gouw, J., Gilman, J. B., Kuster, W. C., and Brown, S. S.: Vertically resolved measurements of

1    nighttime radical reservoirs; in Los Angeles and their contribution to the urban uadical budget, Environmental

2    Science & Technology, 46, 10965-10973, 10.1021/es302206a, 2012.

3    Zhang, N., Zhou, X. L., Shepson, P. B., Gao, H. L., Alaghmand, M., and Stirm, B.: Aircraft measurement of HONO

4    vertical profiles over a forested region, Geophysical Research Letters, 36, 10.1029/2009gl038999, 2009.

5    Zhang, L., Wang, T., Zhang, Q., Zheng, J., Xu, Z., and Lv, M.: Potential sources of nitrous acid (HONO) and their

6    impacts on ozone: A WRF-Chem study in a polluted subtropical region, Journal of Geophysical Research:

7    Atmospheres, 121, 3645-3662, 10.1002/2015JD024468, 2016.

8    Zhou, X. L., Gao, H. L., He, Y., Huang, G., Bertman, S. B., Civerolo, K., and Schwab, J.: Nitric acid photolysis on

9    surfaces in low-NOx environments: Significant atmospheric implications, Geophysical Research Letters, 30,

10    10.1029/2003gl018620, 2003.

11    Zhou, X., Zhang, N., TerAvest, M., Tang, D., Hou, J., Bertman, S., Alaghmand, M., Shepson, P. B., Carroll, M. A.,

12    Griffith, S., Dusanter, S., and Stevens, P. S.: Nitric acid photolysis on forest canopy surface as a source for

13    tropospheric nitrous acid, Nature Geoscience, 4, 440-443, 10.1038/ngeo1164, 2011.

14

15

16

17

18    **Table 1: Overview on the samples, distribution of replicates of soil/biocrust type and the different analysis:**

| Type | Only nutrient analysis | Flux measurements, followed by nutrient and chlorophyll analysis | Sum |
|---|---|---|---|
| Bare soil | 3 | 3 | 6 |
| Dark BSC | 3 | 5 | 8 |
| Light BSC | 3 | 4 | 10 |
| Light BSC + cyanolichen | 3 |  |  |
| Chlorolichen BSC I | 3 | 3 | 12 |
| Chlorolichen BSC II |  | 6 |  |
| Moss BSC | 3 | 4 | 7 |
| sum | 18 | 25 | 43 |

19

20

21

**N$_2$ fixation**
Free living cyanobacteria: e.g. *Nostoc, Scytonema, Spirirestis*
Lichenized cyanobacteria: e.g. *Collema, Leptogium, Lichinella*
Heterotrophic and autotrophic bacteria: e.g. *Azotobacter, Derxia, Beijerinckia*
Vascular plant symbiont: e.g. *Rhizobium, Frankia*

atmosphere



**Nitrification**
heterotrophic and autotrophic bacteria:
e.g. *Nitrosomonas, Nitrosococcus,*
*Nitrobacter, Nitrospina*

**(nitrifier) denitrification**
Fungi and heterotrophic bacteria:
e.g. *Pseudomonas, Alcaligenes,*
*Bacillus, Propionibacterium*

Soil +
biocrusts

1
2     **Fig. 1: Nitrogen cycle at the atmosphere and pedosphere/biosphere interface including nitrogen fixation, nitrification,**
3     **denitrification and emission. Involved enzymes and organisms are specified.**

1
2 **Fig. 2: Climatic conditions of air and soil during April 2016, about one month before samples were taken. Atmospheric**
3 **data was adopted from the Department of Meteorology, Cyprus. Minimum and maximum air temperatures (A) of one day**
4 **at both sites are presented by red and yellow shaded areas. Air-rH data (B; dark blue line, left axis) were only available**
5 **for Paphos airport, representing values at 8:00 and 13:00 local time. Precipitation data at Paphos airport and Prodromos**
6 **(B; blue bars, right axis) show the daily rainfall. Surface temperature and rH are shown on the right side (C, D). The time**
7 **resolution is 5 min. The variations between sensors arise from 3 different locations/surface (bare soil, next to rock, under**
8 **shrubs). (http://www.moa.gov.cy/moa/ms/ms.nsf/DMLmeteo_reports_en/DMLmeteo_reports_en?OpenDocument)**

9



10
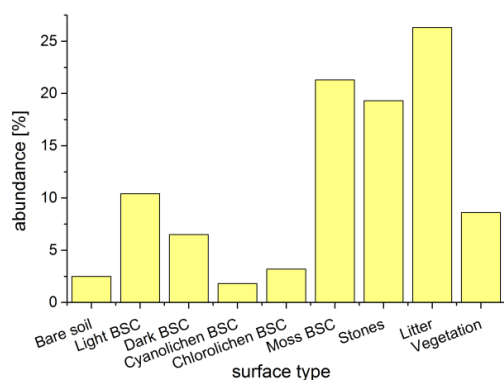
11 **Fig. 3: Distribution of different types of ground surfaces in the studied area. Information derived from 50 grids.**

Atmospheric
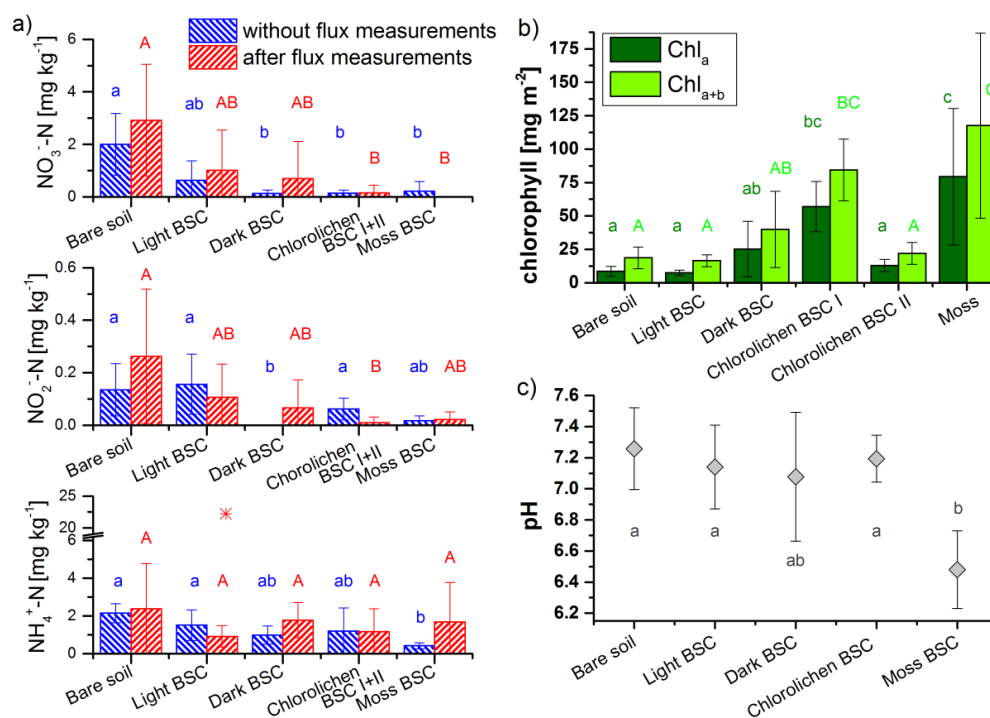Chemistry
and Physics
Discussions



1

Fig. 4: Nutrient- and chlorophyll contents as well as pH values of bare soil and biocrust samples of different types. a)
Nitrate, nitrite and ammonium contents without and after flux measurements. The red star indicates an outlier, b)
Chlorophyll a and chlorophyll a+b contents of samples after flux measurements c) pH values of samples without and after
flux measurements (bare soil and moss BSC: n = 4; light, dark and chlorolichen BSC: n = 3). Number of replicates for a
and b see table 1. In all 3 plots error bars indicate standard deviation and different letters indicate significant differences
(of log-transformed data; p=0.05).

Atmospheric
Chemistry
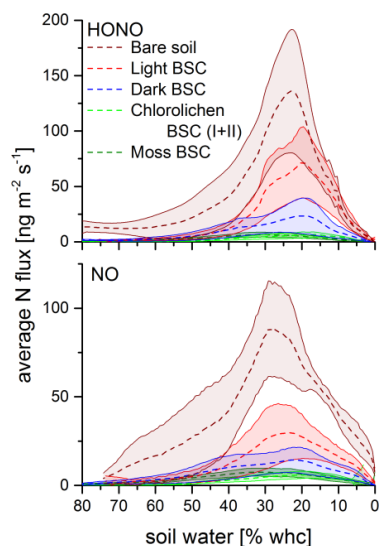and Physics
Discussions
Open Access
EGU

1

Fig. 5: HONO and NO emission fluxes as a function of soil water content. Dotted lines are the mean fluxes. Shaded areas indicate the standard deviation.
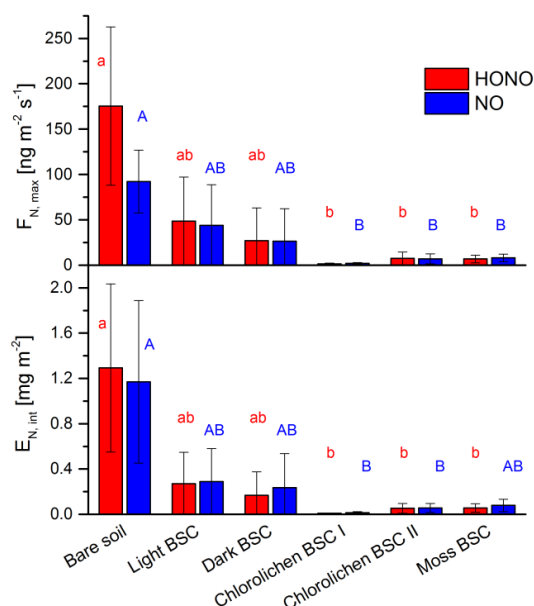
4

5

Fig. 6: Emission of HONO and NO from bare soil and biocrusts. Upper panel: Maximum HONO-N and NO-N fluxes in ng m$^{-2}$ s$^{-1}$ at optimum water conditions; Lower panel: Emissions integrated over a whole wetting-and-drying cycle in mg (N) m$^{-2}$; letters show significant difference (p=0.05,of log-transformed data); error bars indicate standard deviation of replicates (bare soil n=3; light BSC n=4; dark BSC n=5; chlorolichen BSC I n=3; chlorolichen BSC II n=6; moss BSC n=4).
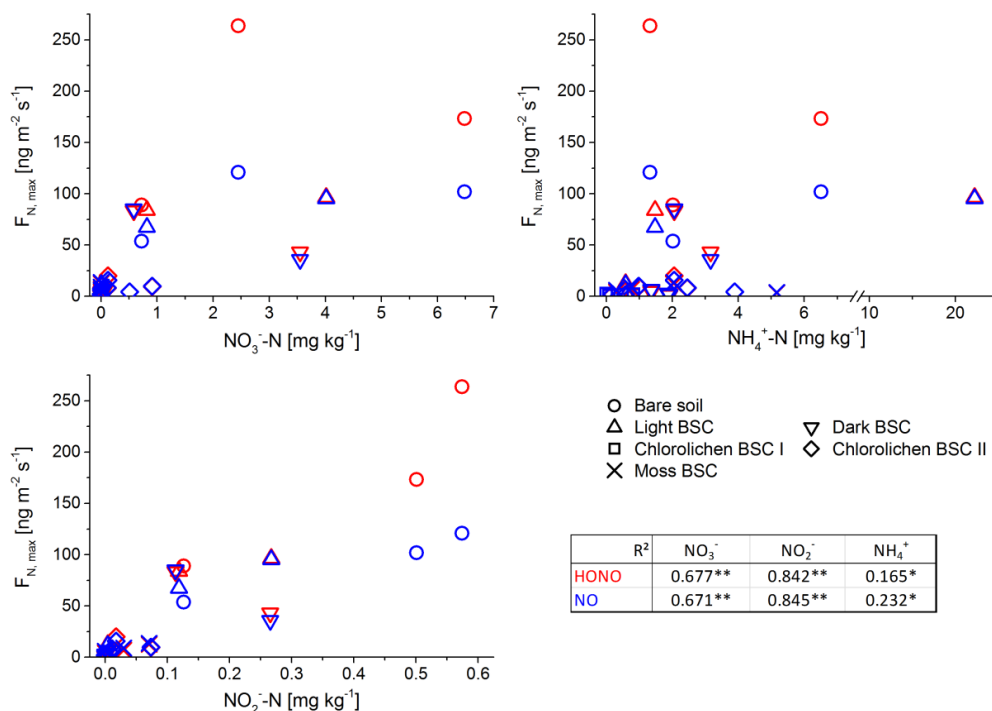
1

2    Fig. 7: Correlation between maximum flux of HONO and NO and nutrient content of all Cyprus soil and biocrust samples
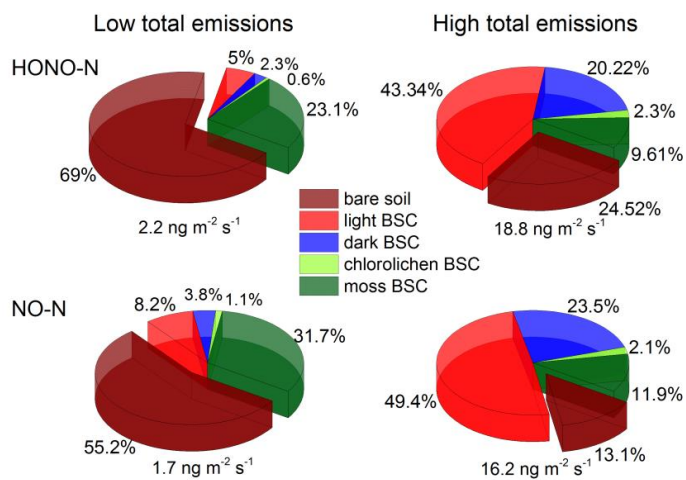3    with Pearson correlation factors (of log transformed data; **: $p < 0.001$; *: $p < 0.05$).

4

5



6

7    Fig. 8: Contributions of different ground surfaces to the total F*.